Protein Patterning by UV-Induced Photodegradation of Poly(oligo(ethylene glycol) methacrylate) Brushes

ARTICLE *in* LANGMUIR · MARCH 2010

Impact Factor: 4.46 · DOI: 10.1021/la100438d · Source: PubMed

Langmuir
Article
pubs.acs.org/Langmuir

Protein Patterning by UV-Induced Photodegradation of Poly(oligo(ethylene glycol) methacrylate) Brushes

Shahrul Alang Ahmad,[†,§] Angus Hucknall,[‡] Ashutosh Chilkoti,*[,‡] and Graham J. Leggett*[,†]

[†]*Department of Chemistry, University of Sheffield, Brook Hill, Sheffield S3 7HF, U.K., and* [‡]*Department of Biomedical Engineering, PO Box 90281, Duke University, Durham, North Carolina 27708-0281.* [§]*Present address: Department of Chemistry, Faculty of Science, Universiti Putra Malaysia, 43400 UPM Serdang, Selangor, Malaysia*

Received January 29, 2010. Revised Manuscript Received March 18, 2010

The UV photodegradation of protein-resistant poly(oligo(ethylene glycol) methacrylate) (POEGMA) bottle-brush films, grown on silicon oxide by surface-initiated atom radical transfer polymerization, was studied using X-ray photoelectron spectroscopy (XPS) and atomic force microscopy (AFM). Exposure to light with a wavelength of 244 nm caused a loss of polyether units from the brush structure and the creation of aldehyde groups that could be derivatized with amines. An increase was measured in the coefficient of friction of the photodegraded polymer brush compared to the native brush, attributed to the creation of a heterogeneous surface film, leading to increased energy dissipation through film deformation and the creation of new polar functional groups at the surface. Exposure of the films through a photomask yielded sharp, well-defined patterns. Analysis of topographical images showed that physical removal of material occurred during exposure, at a rate of 1.35 nm J^{-1} cm^2. Using fluorescence microscopy, the adsorption of labeled proteins onto the exposed surfaces was studied. It was found that protein strongly adsorbed to exposed areas, while the masked regions retained their protein resistance. Exposure of the film to UV light from a scanning near-field optical microscope yielded submicrometer-scale patterns. These data indicate that a simple, rapid, one-step photoconversion of the poly(OEGMA) brush occurs that transforms it from a highly protein-resistant material to one that adsorbs protein and can covalently bind amine-containing molecules and that this photoconversion can be spatially addressed with high spatial resolution.

Introduction

The control of protein adsorption remains a critical challenge in many areas of biotechnology because proteins adsorb strongly and irreversibly to many surfaces. The most widely used protein-resistant materials are ones based on poly(ethylene glycol) (PEG).[1] PEG was one of the first "nonfouling" materials to be identified and remains the prototypical protein-resistant material, although a much larger group of polymers has now been reported to offer similar benefits.[2] While covalent coupling of PEG is the most common route to modifying surfaces to impart protein resistance, the low density of PEG that is typically achieved by covalent immobilization reduces but does not eliminate adsorption of proteins.[3,4] Oligomeric ethylene glycol (OEG) groups attached to alkanethiols provide protein-resistant self-assembled monolayers (SAMs)[5−7] but are limited to gold.

Motivated by the need to develop a robust method that provides protein resistance to a diverse range of materials, Chilkoti and co-workers demonstrated that polymer brushes of oligo(ethylene glycol) methacrylate (OEGMA) synthesized by surface-initiated atom transfer radical polymerization (SI-ATRP) exhibit exceptional resistance to protein adsorption.[4,8−11] In this method, bottle-brush structures are synthesized by in situ ATRP of OEGMA on a surface that is functionalized with a suitable ATRP initiator (usually a bromoisobutyrate group). The initiator can be attached to a wide range of surfaces—to gold via alkanethiol SAM that presents a terminal ATRP initiator,[8] to silicon dioxide by chemisorption of a bromoisobutyrate-terminated silane,[11] or by coupling the initiator to an aminated silane film[12] and on different polymers via plasma deposition or spin- or dip-coating of a halogenated polymers that provides initiation sites for SI-ATRP.[13] This methodology to synthesize protein-resistant polymer coatings is attractive because it appears to translate well to diverse substrates: to date, as it has been successfully applied to gold,[8,9] silicon oxide,[11] and a variety of polymers,[13] it can be carried out under relatively benign conditions (e.g., in water/alcohol mixtures at room temperature) and provides tunable control of the thickness of the polymer brush.

Previous studies have reported methods for the patterning of OEGMA brush growth through prior patterning of ATRP initiators. For example, microcontact printing has been used to pattern the attachment of initiators with terminal thiol functionalities; subsequent ATRP yielded brush structures whose dimensions were defined by the pattern of adsorbed initiator

*Corresponding authors. E-mail: chilkoti@duke.edu (A.C.), Graham.Leggett@shef.ac.uk (G.J.L.).

(1) Harris, J. M. *Poly(Ethylene Glycol) Chemistry: Biochemical and Biomedical Applications*; Plenum: New York, 1992.
(2) Zhou, F.; Huck, W. T. S. *Phys. Chem. Chem. Phys.* **2006**, *8*, 3815.
(3) Michel, R.; Pasche, S.; Textor, M.; Castner, D. G. *Langmuir* **2005**, *21*, 12327.
(4) Hucknall, A.; Rangarajan, S.; Chilkoti, A. *Adv. Mater.* **2009**, *21*, 2441.
(5) Pale-Grosdemange, C.; Simon, E. S.; Prime, K. L.; Whitesides, G. M. *J. Am. Chem. Soc.* **1991**, *113*, 12.
(6) Ostuni, E.; Chapman, R. G.; Holmlin, E. R.; Takayama, S.; Whitesides, G. M. *Langmuir* **2001**, *17*, 5605.
(7) Harder, P.; Grunze, M.; Dahint, R.; Whitesides, G. M.; Laibinis, P. E. *J. Phys. Chem. B* **1998**, *102*, 426.
(8) Ma, H. W.; Hyun, J. H.; Stiller, P.; Chilkoti, A. *Adv. Mater.* **2004**, *16*, 338.
(9) Ma, H.; Wells, M.; T., P. B., Jr.; Chilkoti, A. *Adv. Funct. Mater.* **2006**, *16*, 640.
(10) Ma, H.; Textor, M.; Clark, R. L.; Chilkoti, A. *Biointerphases* **2006**, *1*, 35.
(11) Ma, H.; Li, D.; Sheng, X.; Zhao, B.; Chilkoti, A. *Langmuir* **2006**, *22*, 3751.
(12) Hucknall, A.; Kim, D. H.; Rangarajan, S.; Hill, R. T.; Reichert, W. M.; Chilkoti, A. *Adv. Mater.* **2009**, *21*, 1968.
(13) Hucknall, A.; Simnick, A. J.; Hill, R. T.; Chilkoti, A.; Garcia, A.; Johannes, M. S.; Clark, R. L.; Zauscher, S.; Ratner, B. D. *Biointerphases* **2009**, *4*, FA50.

molecules.[11] At smaller length scales, dip-pen nanolithography has been used in an analogous fashion to deposit initiators in patterns, from which poly(NIPAMM) brushes have been grown.[14] In the present study, the problem has been approached from an opposite perspective, by first forming a complete film of poly(OEGMA) and then seeking to selectively degrade the film to yield protein-binding areas. The approach is inspired by recent work in which oligo(ethylene glycol)-terminated SAMs have been reported to be photodegraded by exposure to UV light with a wavelength of 244 nm,[15−17] yielding surfaces that bind proteins strongly. It has been suggested that UV light causes the breakdown of the OEG chain to yield aldehydes that may covalently bond proteins.[16] In the present work, the photodegradation of poly(OEGMA) films has been investigated using X-ray photoelectron spectroscopy (XPS). The potential offered for the patterning of protein adsorption has been investigated using exposure through a mask to carry out selective area exposure, and the capacity to control protein organization down to small length scales has been examined by using a scanning near-field optical microscope (SNOM) to carry out exposure.

Experimental Section

Materials. Phosphate buffered saline (PBS), 4-(2-hydroxyethyl)piperazine-1-ethanesulfonic acid (HEPES), Alexa Fluor 647 conjugated Streptavidin, and FluoSpheres NeutrAvidin labeled microspheres, 0.04 μm, yellow-green fluorescent (505/515) *1%, were purchased from Invitrogen Molecular Probes. 2-Amino-1,1,1-trifluoroethane (>99%), Streptavidin from *Streptomyces avidinii*, and 5(6)-(biotinamidohexanoylamido)pentylthioureidylfluorescein (≥90%) were obtained from Sigma-Aldrich Chemicals. Immersion oil "Immersol" 518 F, fluorescence free, and Citifluor glycerol/PBS solution fluorescent mountant were purchased from Carl Zeiss and Citifluor Ltd., respectively.

Preparation of Poly(oligo(ethylene glycol) methacrylate) (POEGMA) Brushes. All reagents for the synthesis of the POEGMA brushes were from Sigma-Aldrich. Silicon wafers (University Wafer, Boston, MA) were cleaned in a solution of H_2SO_4:H_2O_2 (3:1) for 30 min. After rinsing with deionized H_2O and drying, the cleaned slides were immersed in aminopropyltriethoxysilane (10%) in ethanol for 30 min and were then rinsed with ethanol and dried at 120 °C for 3 h. Wafers were then immersed in a solution of bromoisobutyryl bromide (1%) and triethylamine (1%) in dichloromethane for 30 min, rinsed with dichloromethane and ethanol, and blown dry with N_2. Wafers were then immersed for 12 h at room temperature in a degassed polymerization solution of Cu(I)Br (5 mg mL^{-1}), bipyridine (12 mg mL^{-1}), and oligo(ethylene glycol) methacrylate, M_n = 360 (300 mg mL^{-1}), under argon (step 3). Finally, wafers were rinsed with deionized H_2O and blown dry with N_2. The thickness of the poly(OEGMA) layer was measured by ellipsometry in air using a M-88 spectroscopic ellipsometer (J.A. Woollam, Lincoln, NE).

Surface Photodegradation and Patterning. A Coherent Innova 300C FreD argon ion laser (Coherent FreD 300C, Coherent U.K., Ely) with an emission wavelength of 244 nm was utilized to carry out polymer photodegradation. The samples were irradiated at a power of 20 mW. The irradiated area was 1.77 cm^2. In order to fabricate POEGMA micropatterns, the surface was irradiated through a Cu electron microscope grid (Agar, Cambridge, UK) that was employed as a mask. Scanning near-field photolithography (SNP) was performed using a Thermo-Microscopes Aurora III NSOM system (Veeco, Cambridge, U.K.). Light from the frequency-doubled argon ion laser was coupled to the end of the fiber probe through an optical coupler at a scan rate of 0.3 μm s^{-1}.

Surface Derivatization. In order to examine the reactivity of the aldehyde generated by UV exposure, the surface was derivatized with 2-amino-1,1,1-trifluoroethane (TFEA). The samples were immersed in a solution of 1 mM TFEA in ethanol for 2 h. After removal, the samples were rinsed with ethanol and dried with nitrogen.

Protein Immobilization. Protein−surface interactions were studied using two systems: FluoSphere NeutrAvidin microspheres (0.04 μm, yellow-green fluorescence) and Alexa-Fluor 647-labeled streptavidin. Both were dissolved in 0.1 M PBS at a concentration of 10 μg mL^{-1}. The samples were immersed in these solutions for 2 h, washed with PBS solution and deionized water, and gently dried with nitrogen, before being characterized using confocal microscopy. To test the retention of functionality by immobilized streptavidin, the sample was first exposed to a solution of streptavidin (10 μg mL^{-1} in 0.1 M PBS) for 2 h, then removed, rinsed with buffer, and dried with nitrogen, before being immersed for 2 h in a 10 μg mL^{-1} solution of 5(6)-(biotinamidohexanoylamido)pentylthioureidylfluorescein in PBS.

Surface Analysis. Advancing sessile drop contact angles were measured on a Rame-Hart model 100-00 goniometer (Netcong, NJ). Topographical atomic force microscopy (AFM) and friction force microscopy (FFM) were performed on a Digital Instruments Nanoscope Multimode IIIa atomic force microscope (Digital Instruments, Cambridge, UK) using silicon nitride nanoprobes (Digital Instruments, Cambridge, UK), operating in air. The nominal normal force constants of these probes were 0.06 or 0.12 N m^{-1}. The degradation of polymer brushes and surface derivatization were quantified using a Kratos Axis Ultra spectrometer (Kratos Analytical, Manchester, UK), equipped with a monochromatized Al Kα X-ray source operating at a power of 150 W. An electron energy analyzer pass energy of 120 eV was used for high-resolution scans, and data were processed using CasaXPS software. All binding energies were referenced to the main hydrocarbon peak, set at a binding energy of 285 eV. Peaks were fit with a linear background, using symmetrical Voigt-type functions, with contributions from both Gaussian and Lorentzian profiles (typically in the proportion 90% Gaussian to 10% Lorentzian).

Fluorescence images were acquired with a LSM 510 meta laser scanning confocal microscope (Carl Zeiss, Welwyn Garden City, UK). The sample was placed on a microscope slide followed by a mount in Citifluor as an antifade reagent (glycerol-PBS solution, AF1) (Citifluor Ltd., London, United Kingdom). 40× and 63× magnification oil dipping lens were used for imaging with numerical apertures of 1.30 and 1.40, respectively. A small drop of immersion oil (Immersol 518 F, Zeiss) was placed on the slide in the center of the illuminated area. The 488 and 633 nm bands of Ar and HeNe lasers were used to excite the yellow-green fluorescent of NeutrAvidin and Alexa Fluor 647 conjugated-Streptavidin, respectively, and the fluorescence was collected at wavelengths above 515 and 670 nm. Band filters operating between 500 and 550 nm and 650−710 nm were used, respectively. The fluorescence images were analyzed using Zeiss LSM image browser software.

Results and Discussion

X-ray Photoelectron Spectroscopy. Figure 1a shows the C 1s region for the virgin POEGMA brush film. The dominant component at 286.7 eV binding energy corresponds to the ether carbon atoms in the oligo(ethylene glycol) brush. In addition, small amounts of aliphatic carbon (285.0 eV) and carboxylate carbon (289.2 eV) are also observed.

Figure 1b shows the C 1s spectra of POEGMA brushes on silicon oxide that were exposed to a range of doses of UV

(14) Kaholek, M.; Lee, W.-K.; LaMattina, B.; Caster, K. C.; Zauscher, S. *Nano Lett.* **2004**, *4*, 373.
(15) Montague, M.; Ducker, R. E.; Chong, K. S. L.; Manning, R. J.; Rutten, F. J. M.; Davies, M. C.; Leggett, G. J. *Langmuir* **2007**, *23*, 7328.
(16) Ducker, R. E.; Janusz, S. J.; Sun, S.; Leggett, G. J. *J. Am. Chem. Soc.* **2007**, *129*, 14842.
(17) Reynolds, N. P.; Tucker, J. D.; Davison, P. A.; Timney, J. A.; Hunter, C. N.; Leggett, G. J. *J. Am. Chem. Soc.* **2009**, *131*, 896.

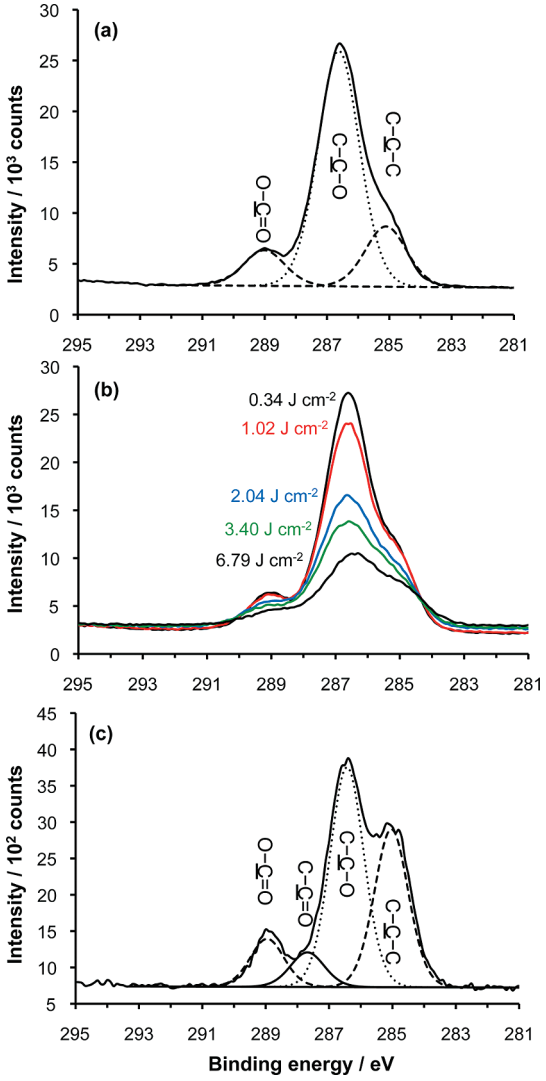

Figure 1. (a) C 1s spectrum of a virgin POEGMA brush sample. (b) Variation in the C 1s spectrum with exposure to UV light. (c) C 1s spectrum after exposure to 5.43 J cm^{-2} showing peak fits, including the aldehyde component at 288 eV.

irradiation (λ = 244 nm). Significant changes were observed in their C 1s spectra. The peak intensity of the C 1s spectrum decreased with exposure, suggesting that the thickness of the brush decreased with increasing UV dose. The largest change was in the relative contribution of the ether component, which decreased markedly not only in its absolute area but also in its area relative to those of the other components in the spectrum. Although the peak area of the other components also reduced after exposure, the change was much less significant than was the case for the ether component. Additionally, a new component was observed at 288 eV which was attributed to the formation of aldehyde species at the surface. In previous studies of SAMs of OEG-terminated thiols, it has been reported that photodegradation of the OEG chain leads to a reduction of the area of the ether component in the C 1s region and the appearance of a new carbonyl component at ca. 288 eV, attributed to the formation of aldehyde groups.[15−17] The present data suggest that similar changes occur following UV irradiation of POEGMA brush films.

Photodegradation was also attempted using an alternate light source, an HeCd laser emitting at 325 nm. No photodegradation was observed, suggesting that the process is wavelength-dependent:

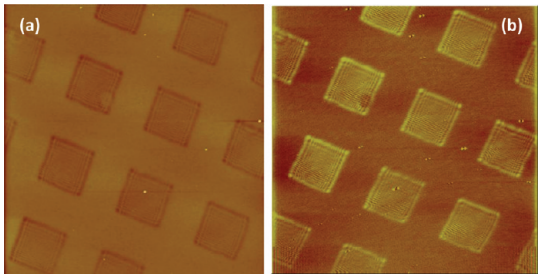

Figure 2. 50 × 50 μm^2 AFM topography (a) and friction (b) images of POEGMA brush samples following exposure to UV light through a mask. *Z*-ranges: (a) 0−50 nm; (b) 0−3.0 V.

photons with longer wavelengths may not have sufficient energy to initiate bond breaking in the POEGMA film.

Atomic Force Microscopy. Samples were exposed to UV light through masks and imaged by atomic force microscopy (AFM). Figure 2 shows a sample that was exposed to a dose of 5.43 J cm^{-2}. Friction images were acquired by subtracting the lateral force images in the forward and reverse directions to remove topographical contributions to the contrast.[18−20] Following exposure, significant changes were observed in both the topographical and the friction images. Figure 2a shows the surface topography. In the exposed regions (squares), the contrast is darker than the masked areas, indicating that they are lower, meaning that material is removed from the brush in these regions during the degradation process. As no washing step was used after UV exposure, this means that some of the products of the degradation process are volatile. The line section shows that the mean height difference between the masked and the exposed areas is 8.26 ± 0.31 nm. The original, unexposed film had a thickness of 140 nm.

In the friction image (Figure 2b), the exposed regions exhibit brighter contrast than the masked ones, indicating that the friction force is larger in the exposed regions than in the masked areas. The difference in the frictional contrast observed in the exposed and masked regions may be attributed to two effects. First, the reduction in the brush length as a result of photodegradation causes heterogeneity in the brush layer, which in turn means that the energy barrier to chain conformational change is reduced.[21] Consequently, there are additional pathways for energy dissipation in the sliding contact and hence a larger frictional force in the UV-exposed and degraded regions of the polybrush. Second, the creation of greater numbers of polar functionalities may yield an additional adhesive contribution to the frictional force (e.g., through energy dissipated in shearing adhesive tip−sample interactions).[22,23]

Figure 3 shows the variation in the height difference and friction signal between the exposed and masked regions as a function of the UV exposure. It can be seen in Figure 3a that the height difference between the masked and exposed regions increased monotonically as a function of exposure. After an exposure of 10 J cm^{-2}, the depth of material eroded from the exposed regions was ca. 13.5 nm, so that the mean erosion rate was 1.35 nm J^{-1} cm^2. This represents a rapid removal of material. The extent of change is further illustrated by the development of

(18) Grafstrom, S.; Neitzert, M.; hagen, T.; Ackerman, J.; Neumann, R.; Probst, O.; Wortge, M. *Nanotechnology* **1993**, *4*, 143.
(19) Carpick, R. W.; Salmeron, M. *Chem. Rev.* **1997**, *97*, 1163.
(20) Gnecco, E.; Bennewitz, R.; Gyalog, T.; Meyer, E. *J. Phys.: Condens. Matter* **2001**, *13*, R619.
(21) Beake, B. D.; Leggett, G. J. *Langmuir* **2000**, *16*, 735.
(22) Beake, B. D.; Leggett, G. J. *Phys. Chem. Chem. Phys.* **1999**, *1*, 3345.
(23) Brewer, N. J.; Beake, B. D.; Leggett, G. J. *Langmuir* **2001**, *16*, 735.

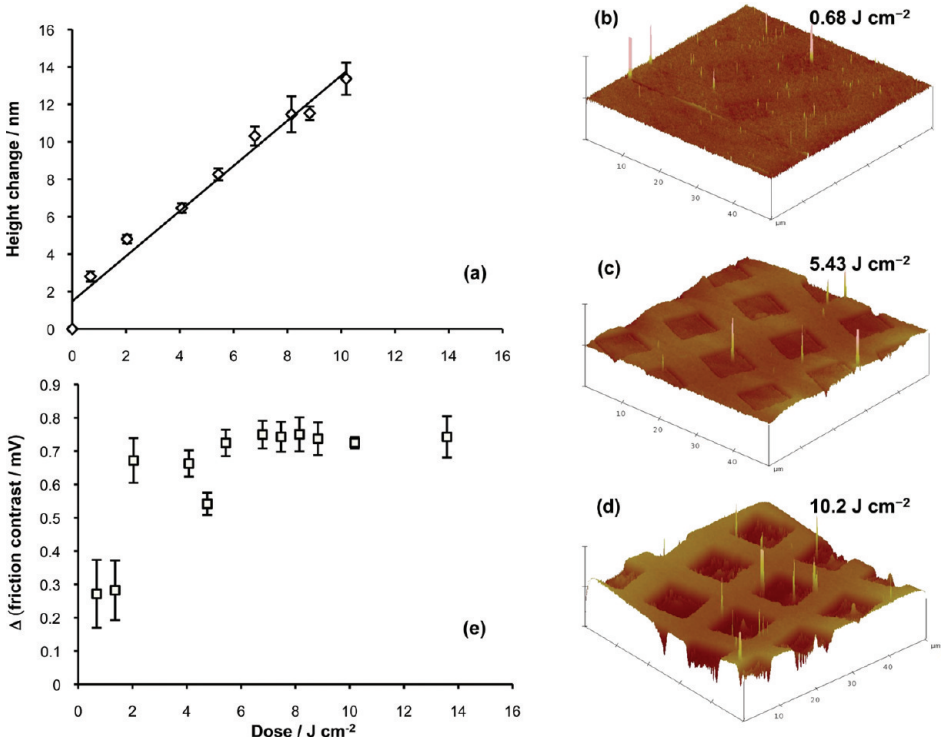

Figure 3. Difference in (a) height and (b) friction contrast between masked and exposed areas as a function of dose for POEGMA brush samples exposed to UV light through a mask. Images (b) to (d) show 50 × 50 μm^2 AFM topographical images, with a common vertical range of 35 nm, as a function of UV exposure.

the surface topography as shown in Figure 3b−d. All three images have been normalized to the same vertical range (35 nm); it is clear that the topography develops rapidly. In contrast, the friction difference between the masked and exposed regions increased up to an exposure of ca. 2 J cm^{-2}, whereafter the value remained constant. The attainment of a constant frictional difference for larger exposures suggests that the composition and the molecular structure in the exposed areas reached a steady state within the depth sampled by the AFM, probably when all the chains had become at least partly degraded, and that this equilibrium molecular structure changed little as material was subsequently removed from the surface (until eventually the brush is removed completely from the underlying substrate).

While the data in Figure 3a suggest that ca. 10% of the film thickness is lost after a dose of ca. 10 J cm^{-2}, the XPS data in Figure 1b suggest that the change is greater. The reason for this difference is not clear. One possibility is that the photodegradation process produces substantial volumes of low-molecular-weight material that are removed under vacuum or easily displaced under the influence of the X-ray beam.

Because the XPS data suggested that aldehyde functional groups were created by UV exposure, as was previously reported in UV studies of photodegradation of OEG-terminated SAMs on gold surfaces, the reactivity of photochemically modified surfaces with a fluorinated amine was tested. Figure 4 shows the C 1s, N 1s, and F 1s spectra of samples exposed to a UV dose of 5.43 J cm^{-2}, before and after subsequent exposure of the sample to a solution of trifluoroethylamine. It can be seen from the XPS spectra that there was no nitrogen or fluorine in the sample before exposure to the trifluoroethylamine solution. After exposure, there were clear N 1s and F 1s peaks, and a new peak appeared at a binding energy of 293.2 eV in the C 1s spectrum, corresponding to a carbon atom bonded to three fluorine atoms in the amide product of the derivatization reaction. This peak is small, but given the thickness of the brush film (which extends throughout the XPS sampling depth), this is as expected. These data clearly indicate that the reactivity of the surface is changed by UV exposure and support the conclusion that aldehyde groups are introduced as a consequence of the degradation reaction and that these remain available for binding of molecules to the brush film. Control samples that had not been exposed to UV light also exhibited no uptake of reagent (i.e., no peaks were observed in the N 1s and F 1s regions).

Protein Adsorption. POEGMA films exhibit exceptional resistance to protein adsorption.[8,9,11] Given that UV exposure causes degradation of the brush molecular structure and leads to the introduction of carbonyl and carboxylate groups to the surface, we hypothesized that there should also be a reduction in the protein resistance of exposed areas of brush films. Figure 5 shows confocal fluorescence images of a control (unexposed) sample (a) and a sample exposed to a dose of 5.43 J cm^{-2} through a mask (b) following immersion of both samples in a solution of FluoSphere NeutrAvidin labeled microspheres (0.04 μm, yellow-green fluorescence). No fluorescence is seen in Figure 5a, indicating that the film is, within the limits of sensitivity of fluorescence microscopy, resistant to the adsorption of the protein-coated nanospheres. In contrast, in Figure 5b, strong fluorescence is observed from the square regions, which were exposed to UV light through the mask, indicating that UV modification of the brush abrogated its protein resistance, as seen by the avid adsorption of Neutravidin particles to the photodegraded regions of the POEGMA brush. Parts c and d of Figure 5 show images acquired for similar patterned samples following immersion in respectively solutions of FITC-labeled IgG and Alexa-Fluor 633 labeled streptavidin. In each case, there is plainly dark contrast from the bars (masked regions), indicating retention of resistance to protein adsorption in those areas (within the limits of sensitivity of fluorescence microscopy), and bright fluorescence from the square, exposed areas, indicating that protein adsorption has occurred there.

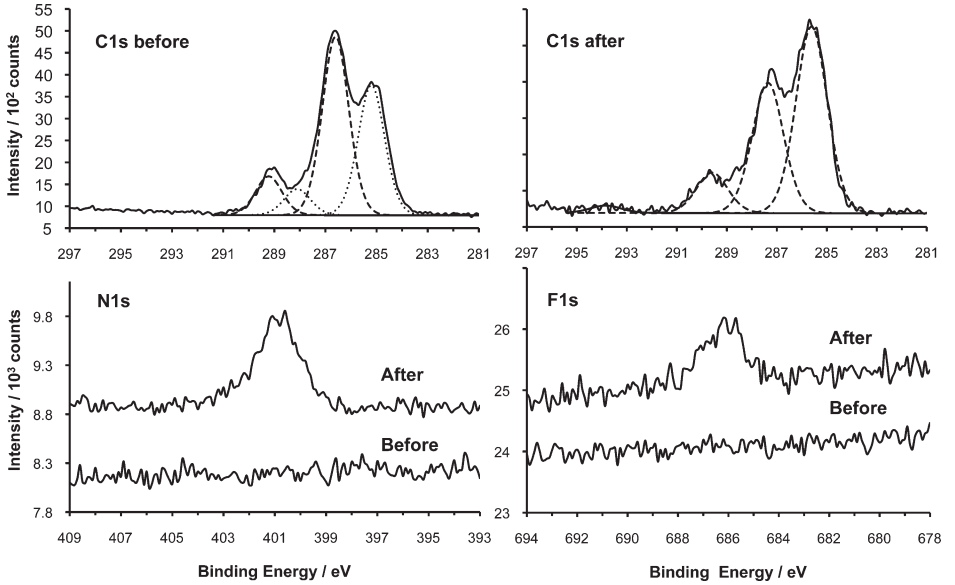

Figure 4. C 1s, N 1s, and F 1s regions of the XP spectra of POEGMA brush samples exposed to UV light, before and after exposure to a solution of trifluoroethylamine.

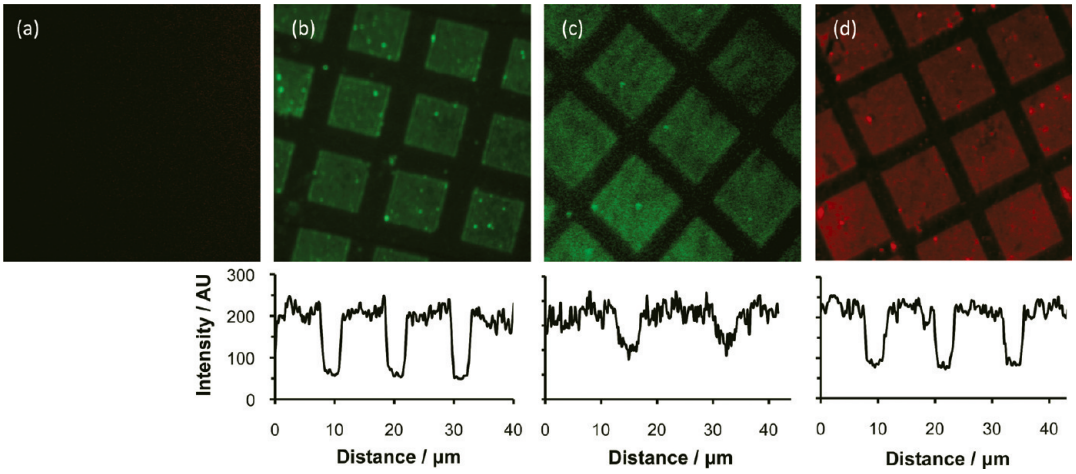

Figure 5. Fluorescence micrographs showing (a) control and (b) patterned POEGMA brush sample following immersion in a solution of NeutrAvivin nanoparticles. (c) Patterned sample following immersion in a solution of FITC-labeled IgG. (d) Patterned sample following immersion in a solution of Alexa-Fluor 633-labeled streptavidin. Images sizes: 42 × 42 μm^2. A representative cross section through the fluorescence image is shown for each of (b) to (d).

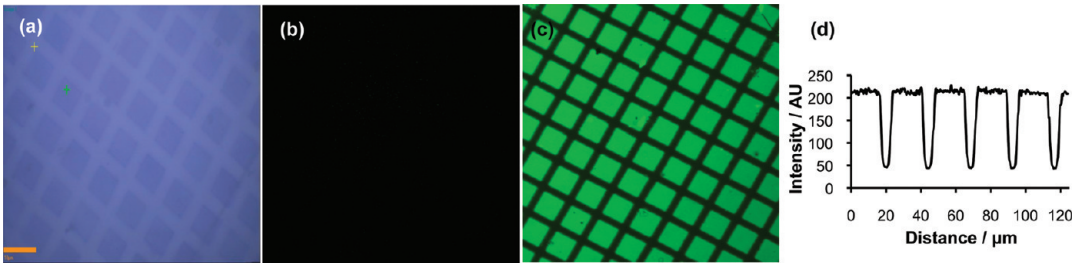

Figure 6. (a) Optical micrograph of a patterned POEGMA brush sample following immersion in a solution of unlabeled streptavidin. (b) Corresponding fluorescence image. (c) Fluorescence image following subsequent exposure to a solution of FITC-labeled biotin. (d) Cross section through (c). Image sizes in (a) to (c): 205 × 205 μm^2.

Figure 6 shows images of a sample that has been exposed to UV light through a mask and then immersed in a solution of unlabeled streptavidin. An optical micrograph shows faint contrast in the exposed regions (a), suggesting that the UV modification followed by protein adsorption has modified the optical properties of the surface in those regions. However, no fluorescence contrast is observed from the same area (b). Following immersion of the sample in a solution of FITC-labeled biotin, bright fluorescence is

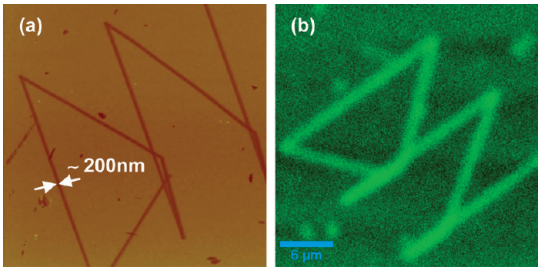

Figure 7. (a) 24 × 24 μm^2 AFM height image of a POEGMA brush sample that has been patterned by exposure to a near-field probe. (b) Fluorescence microscopy image of a similar sample following exposure to a solution of NeutrAvidin nanoparticles. The scale bar represents 6 μm.

observed from the square regions, indicating not only that streptavidin is adsorbed only onto the exposed areas of the sample but also that following adsorption to the surface it retains its recognition of biotin.

Figure 7a shows a sample that was patterned not by exposure to light through a mask but to the evanescent field associated with a scanning near-field optical microscope (SNOM) probe. A frequency-doubled Ar ion laser (244 nm) emitting at a power of 6 mW was coupled to the SNOM (a Veeco Aurora III system, based around an optical fiber probe controlled in shear-force mode). The probe was traced across the sample surface at a speed of 0.3 $\mu m\ s^{-1}$, and where it traveled, the excitation caused by interaction with the evanescent field caused photochemical modification of the brush surface. The image in Figure 7a is an AFM height image. There is clear topographical contrast, resulting from the fact that while the near-field probe modifies the sample, it also removes material. Analysis of a line section through the image indicates that the depth of the feature was 9.59 ± 0.25 nm. Removal of a similar depth of material during the equivalent micropatterning experiment (Figure 3a) would require an exposure of ca. 7−8 J cm^{-2}, more than sufficient to cause maximum change in the surface composition as measured by FFM (Figure 3b). These data indicate that extensive modification to the surface can be readily accomplished at high resolution using a near-field probe as the light source. Because of the comparative bluntness of the near-field probe, features such as those in Figure 7a could not be fabricated by "scratching" as a result of the shear force because scratching yields poorly defined features, often consisting of multiple, parallel features. In contrast, the lines in Figure 7a are sharply defined.

The line width for the sample shown in Figure 7a was ca. 200 nm. In part this resolution was determined by the diameter of the aperture on the near-field probe. However, the brush here has significant thickness (140 nm), and there is good evidence from modeling that the near-field diverges rapidly in the dielectric layer beneath it in such circumstances, with the consequence that the area perturbed is larger than might otherwise be expected. In view of this, the resolution here probably does not represent the optimum level of performance: it may be possible to write smaller structures by increasing the scan speed and/or the laser power coupled to the probe.

Figure 7b shows a fluorescence image following immersion of a nanopatterned sample in a solution of NeutrAvidin particles. The lines are clearly distinguished from the background material despite their narrow width, exhibiting a strong contrast difference. The line width (325 nm) appears broadened, but this is simply a consequence of the limited resolution of a far-field optical technique.

Conclusions

UV photodegradation of poly(OEGMA) bottle-brush films offers a rapid, simple, one-step route to the conversion of exceptionally protein-resistant surfaces to ones that bind amine-containing molecules (for example, proteins) in a highly spatially selective fashion. Exposure of the brush film causes degradation of the ether units, leading to physical degradation of the film at a rate of 1.35 nm $J^{-1}\ cm^2$. The exposed areas contain aldehyde groups that form bonds to amines, presumably through imine bond formation. The surface degradation yields a more heterogeneous surface, reflected in the increased coefficient of friction following exposure. Comparison of FFM and AFM topographical data suggests that the surface composition achieves a steady state after an exposure of ca. 2 J cm^{-2} but that the surface continues to be physically degraded thereafter. Exposure of the films through a mask yields sharp, well-defined patterns that may be used to pattern the adsorption of labeled proteins and protein-functionalized polymer nanoparticles. The masked regions of the film retain their protein resistance, while the exposed areas adsorb proteins. The use of a scanning near-field optical microscope to carry out the UV degradation process yields submicrometer patterns.

Acknowledgment. S.A.A. thanks the Malaysian Government for a research scholarship. G.J.L. and S.A.A. thank RCUK (grant EP/C523857/1), EPSRC, and the RSC Analytical Chemistry Trust Fund for support.